Document downloaded from:

http://hdl.handle.net/10251/165718

This paper must be cited as:

Bori, L.; Paya-Bosch, E.; Alegre, L.; Viloria, T.; Remohí, J.; Naranjo Ornedo, V.; Meseguer, M. (2020). Novel and conventional embryo parameters as input data for artificial neural networks: an artificial intelligence model applied for prediction of the implantation potential. Fertility and Sterility. 114(6):1232-1241. https://doi.org/10.1016/j.fertnstert.2020.08.023

The final publication is available at

https://doi.org/10.1016/j.fertnstert.2020.08.023

Copyright Elsevier

Additional Information

RUNNING TITLE

Novel markers of embryo implantation

TITLE

Novel and conventional embryo parameters as input data for Artificial Neural Networks: An Artificial Intelligence model applied for prediction of the implantation potential.

AUTHOR NAMES AND AFFILIATIONS

Lorena Bori, MSc[1*]; Elena Paya, MSc[1,2]; Lucia Alegre, MSc[1]; Thamara Alexandra Viloria, PhD[1]; Jose Alejandro Remohi, MD, PhD [1]; Valery Naranjo PhD[2]; Marcos Meseguer PhD[1,3]

[1] IVIRMA Valencia, Spain.

[2] Instituto de Investigación e Innovación en Bioingeniería (I3B), Universitat Politécnica de Valencia, Spain.

[3] Health Research Institute la Fe, Valencia (Spain)

*Correspondence address. IVI Valencia, Pl. Policia Local, 3, Valencia, Spain.

Email: lorena.bori@ivirma.com

Phone number: +34 610 55 37 99

CAPSULE

Novel embryo development parameters analyzed by time-lapse technology are used as input data for a predictive model of implantation potential based on artificial intelligence.

ABSTRACT

Objective: To describe novel embryo features capable of predicting implantation potential used as input data for an artificial neural network (ANN) model.

Design: Retrospective cohort study.

Setting: University-affiliated private IVF center.

Patients: This study included 637 patients from the oocyte donation program who underwent single blastocyst transfer during two consecutive years.

Intervetion(s): None

Main Outcome Measure(s): The research was divided into two phases. Phase 1, consisting of the description and analysis of the following embryo features in implanted and non-implanted embryos: distance and speed of pronuclear migration, blastocyst expanded diameter, inner cell mass area and trophectoderm cell cycle length. Phase 2, consisting of the development of an ANN algorithm for implantation prediction. Results were obtained for four models fed with different input data. The predictive power was measured using the area under the curve (AUC) of the receiver operating characteristic (ROC) curve.

Results: Out of the five novel described parameters, blastocyst expanded diameter and trophectoderm cell cycle length had statistically different values in implanted and non-implanted embryos. After the ANN models were trained and validated using 5-fold cross-validation, they were capable of predicting implantation on testing data with an AUC of 0.64 for ANN1 (conventional morphokinetics), 0.73 for ANN2 (novel morphodynamics), 0.77 for ANN3 (conventional morphokinetics + novel morphodynamics) and 0.68 for ANN4 (discriminatory variables from statistical test).

Conclusion (s): The novel proposed embryo features affect the implantation potential and their combination with conventional morphokinetic parameters is effective as input data for a predictive model based on artificial intelligence.

KEY WORDS: embryo parameters, implantation, Artificial Intelligence, time-lapse, Artificial Neural Network.

INTRODUCTION

The European IVF-monitoring Consortium (EIM) for the European Society of Human Reproduction and Embryology (ESHRE) recorded in the 18th annual report, more than 8 million treatments with Assisted Reproductive Technology (ART) and nearly 1.5 million newborn children (1). Most treatments reported to EIM were performed through Intracytoplasmic Sperm Injection (ICSI) and subsequent in vitro embryo culture. The selection of the most appropriate embryo of an entire cohort is a relevant factor for the successful outcome of an infertility treatment.

From the very beginning of the In Vitro Fertilization (IVF), morphology has been the criterion par excellence to evaluate the development of the embryo (2). The assessment is usually performed under an optical microscope at x400 magnification to count the number of cells, fragmentation level or multinucleation, among other parameters. Limitations of this method are not only associated with the subjectivity of the embryologist (3) but also, with the evaluation per se. Even though the incubator has optimal culture conditions, gas concentrations and temperature are altered by removing the embryos from the incubator to allow a static observation (4). Therefore, embryos are evaluated in punctual occasions and a lot of information is missing among observations (5). It is well reported that the embryo stage and classification can vary in few hours (6,7), resulting in non-successful embryo selection.

The introduction of time-lapse (TL) systems in IVF laboratories allows the continuous monitoring of embryo development in real time. This technology has become a useful tool to study the dynamic embryo development without disturbing the culture conditions and offering objective and precise information in a qualitative and quantitative way (8). It has been used to create predictive algorithms by applying morphological and morphokinetic parameters to choose the best embryo to transfer (9).

Abnormal division patterns, multinucleation, fragmentation or collapse are some of the deselecting parameters used to categorize embryo quality (10). These parameters have been associated with inadequate blastocyst formation (11), low eupolid rate (12) and poor implantation and live birth rate (12–20).

Over time, the final goal of the algorithms has changed from appropriate embryo development to healthy live birth. The most used morphokinetic parameters to predict

blastulation were the duration of the second cell cycle (cc2), the time period to complete synchronous divisions (s2 and s3), the division time to two cells (t2) and the division time to five cells (t5) (13,21–28). The events more frequently used to predict implantation were cc2, t5 and s2 (13,28–32). Even though morphokinetic parameters are not enough to predict ploidy (33), most of the embryos with abnormal cell division times have chromosomal alterations (5,29,34). It is also reported that aneuploid embryos are delayed compared to euploid ones in different morphokinetic parameters, such as the timing of morula and blastocyst formation (35–37). Therefore, TL technology could reduce the risk of transferring aneuploid embryos in treatments with no Preimplantation Genetic Testing (PGT) (38).

Nevertheless, there has been very little improvement in live birth rate over the last few years (1,39), raising the need to investigate new approaches. The continuous recording of the embryo development provides high quality images that allow the embryologists to find precise markers to determine embryo quality.

The problem of the existing algorithms is the incapacity of using the large amount of data provided by time-lapse systems. The innovative artificial intelligence (AI) techniques are capable of changing the subject of study from limited independent variables to Big Data. The AI could be defined as the development of algorithms with the capacity of creating learned models and exercising an intelligent behavior (40). The supervised machine learning is the AI methodology that uses mathematical techniques to give the computer systems the ability to learn from labelled data and make a prediction. The techniques most used in this field are the Artificial Neural Networks (ANNs) such as Convolutional Neural Network (41) or Multilayer Perceptron (42). Recently, the introduction of ANNs in the assisted reproduction investigations has increased seven-fold (43) with promising results (44,45).

The main aim of the present study was to predict embryo implantation potential using novel non-invasive parameters observed by TL monitoring systems. In order to achieve this objective, we proposed new embryo morphodynamic parameters, which had not been evaluated so far by TL, and analyzed their association with the implantation probability. Finally, we developed a model using an artificial neural network to predict the implantation success.

MATERIAL AND METHODS

Study population

This research is a single-center retrospective study carried out at IVI Valencia (Spain). We included recipients from the oocyte donation program who underwent ICSI cycles without PGT from the last two consecutive years. The exclusion criteria for recipients were: uterine pathologies, endometriosis, polycystic ovary syndrome or more than 30 kg/m^2 of Body Mass Index (BMI). Out of the 8.832 treatments with these characteristics, 845 were included in the TL system EmbryoScope Plus™ (Vitrolife, Denmark). Single fresh embryo transfers were performed in 637 of them, whose embryos were assessed in this project.

Ovarian stimulation and uterine receptivity

Donors were stimulated using the conventional controlled ovarian stimulation protocol with gonadotropin-releasing hormone (GnRH) agonist treatment. GnRH agonist (Decapeptyl 1, Ipsen Pharma, Spain) was administered by intramuscular injection until more than eight follicles had reached a mean diameter of ≥18mm. Transvaginal oocyte retrieval was scheduled 36 hours later. The endometrial preparation of patients was undertaken using the hormone replacement therapy described by Cerrillo et al. 2017(46). After embryo transfer, oocyte recipients received a daily dose of 400 mg of vaginal micronized progesterone (Progeffik, Lab. Effik, Madrid, Spain) every 12 hours as luteal phase support.

Oocyte retrieval and ICSI

Transvaginal oocyte retrieval was performed through follicular aspiration and oocytes were washed in gamete medium (Cook Medical®, Australia). Then, oocytes were cultured in fertilization medium (Origio, Cooper Surgical®, Denmark) at 5%CO2, 5%O2 and 37ºC. Denudation was carried out just before ICSI, 4 hours after oocyte retrieval, by mechanical and chemical procedures (pipetting in 40 IU/mL hyaluronidase). ICSI was performed at x 400 magnification with the use of an Olympus IX7 microscope. Finally, oocytes were placed in preequilibrated EmbryoSlides® (Vitrolife, Denmark) with 16 microwells divided into two groups, with 90 µl of single-step medium (Gems, Genea Biomedx®, Australia) per group and 1.6 mL mineral oil per dish.

Embryo incubation, scoring and selection

Embryos were cultured in the TL system EmbryoScope Plus™ up to the blastocyst stage. Images were taken automatically every 10-20 minutes and in up to eleven focal planes. Embryo development was assessed on an external computer with software for the analysis (EmbryoViewer™ workstation, Vitrolife, Denmark). Fertilization was evaluated at 16-19 hours post-ICSI and confirmed by the presence of two pronuclei and two polar bodies. The number of cells, fragmentation level, symmetry among blastomeres and compaction degree were annotated on day 2 and 3 of development. Later, blastocysts were assessed and selected by applying a hierarchical classification procedure based on a combination of standard ASEBIR's morphological grading (Supplemental table 1, Supplemental table 2 and Supplemental table 3) and KIDScore™ D5 algorithm (EmbryoViewer™ software, Vitrolife, Denmark). Embryos were graded from A (high morphological quality) to D (low morphological quality) by senior embryologists and scored from 1 (low likelihood of implantation) to 9.9 (high likelihood of implantation) by the KIDScore D5 ™. The embryo with the highest score among those with good quality morphology was selected to transfer in each treatment. Implantation of transferred embryos was confirmed by ultrasound scanning for gestational sacs with fetal heart beat after 8 weeks of pregnancy.

Experimental design

The project was divided into two phases:

Phase 1. Analysis of novel morphokinetic parameters: distance and speed of pronuclear migration (PNm), inner cell mass area (ICMa), blastocyst expanded diameter (BEd) and trophectoderm cell cycle (ccTroph) length. Not all the parameters could be analyzed on the total of transferred embryos, due to image failures such as darkness, presence of bubbles or out of focus images. The measurements were carried out by a designated embryologist, who was responsible for the annotation of morphokinetic variables (to avoid inter-operator variations), with the drawing tools provided by the EmbryoViewer™ (Vitrolife, Denmark). The distance of PNm was assessed drawing a line from the point of PN juxtaposition up to the position where pronuclei faded, in 505 embryos (Figure 1A). The speed of PNm was calculated using the distance and the duration of this movement. The BEd was measured in 451 embryos in their maximum expansion and always before the embryo started hatching (Figure 1B). The ICMa was evaluated with a circle surrounding its perimeter when the ICM was compacted, in 477

embryos (Figure 1C). To normalize data of BEd and ICMa in early and delayed embryos, we calculated a ratio with the time when the annotations were performed: BEd/tBEd and ICMa/tICMa. The ccTroph length was measured in 360 embryos. We selected one cell and made two marks, the first one when this cell divided into two daughter cells and the second one, when one of the daughter cells divided again (Figure 1D). Subtracting these two division times, we obtained cell cycles lengths in the trophectoderm.

Phase 2. Development of the predictive model based on Artificial Neural Networks (ANN). Novel morphodynamical parameters (distance and speed of PNm, BEd, ICMa and ccTroph) and conventional morphokinetic parameters (the time of the second polar body emission, tpb2; the time of appearance of the two pronuclei, tPNa; the time of their fade out, tPNf; the division time to two cells, t2; the division time to three cells, t3; the division time to four cells, t4; the division time to five cells, t5; the division time to six cells, t6; the division time to seven cells, t7; the division time to eight cells, t8; the time from ICSI to early compaction, tSC; the time of the morula formation, tM; the time to early blastulation, tSB; the time to full blastocyst, tB; the time to expanded blastocyst, tEB; and the time to early hatching blastocyst, tHiB) were considered to develop the model.

The ANN designed was a multilayer perceptron (MLP) and it involved the selection of several hyperparameters. The number of hidden layers and the number of hidden neurons were chosen empirically but starting from rule-of-thumb methods. Firstly, one or two hidden layers should be enough to solve any non-linear complex problem (47). In the present work, the selection of two hidden layers improved model performance. Secondly, the number of hidden layers neurons should be 2/3 of the size of the input layer (48,49). The best model was designed with 15 neurons in each hidden layer (Supplemental figure 1). Too many neurons can result in overfitting problems and not lead to correct generalization.

Initially, the data was pre-processed by cleaning the database (removing samples with more than 5 missing values). Then, filling missing values with different techniques and standardizing the variables through *Z Score*. Conventional variables were temporal dependent. Therefore, we could approximate missing values by interpolation. Novel variables were filled by using their corresponding mean. In this way, 451 embryos were considered to feed ANNs. Afterwards, the parameters were randomized and split into

two groups, 85% for the learning process (training and validation) and 15% for the blind test. In the learning process, the ANN was fed with the input data, the prediction was calculated, and the error was obtained by comparing the output value with the target value. Then, the backward propagation of the error allowed for the model parameter updates. A 5-fold cross-validation approach was performed in order to guarantee robustness to the model (50). In this way, the learning data was divided into 5 sets and the network was trained and validated with different sets of data in each iteration. Finally, the model was tested with the 15% of embryos, which were unknown for the model. It took the embryo parameters as input data and generated a confidence score, ranging from 0 to 1. Using the probability of belonging to each class, the sample was assigned to the majority class.

The ANN was trained and tested by using distinct groups of variables resulting in four models with the same architecture and different input data: conventional morphokinetic parameters for ANN1, novel morphodynamical parameters for ANN2, conventional and novel parameters for ANN3 and those parameters which had significant differences between implanted and non-implanted embryos for ANN4.

Statistical analysis

The discriminatory capacity of each variable and the correlation among them was analyzed. Statistical tests were applied to probe significant differences in the values of each variable between implanted and non-implanted embryos. T-test was used for parameters with normal distribution and Wilcoxon Rank Sum test for those with non-normal distribution. The subsequent results were expressed in terms of the 95% of Confidence Interval and significance. Also, a study of the correlation for each pairwise variable combination was performed. The Pearson's correlation coefficients and their respective p-values were obtained to test the null hypothesis that they are independent. Finally, Receiver Operator Characteristic (ROC) curves were used to analyze the predictive power of the ANN. The resulting graph represents the ratio of true test positives to total positive (sensitivity) per the proportion of false positives (1-specificity). The higher the area under de curve (AUC), the more balanced the compensation between sensitivity and specificity. As a measure of the model performance, we also used the combined metric F-Score which considered the predictive positive values and the sensitivity.

Ethical approval

The procedure and protocol were approved by an Institutional Review Board (IRB reference: 1709-VLC-094-MM), which regulates and approves database analysis and clinical IVF procedures for research at IVI. Additionally, the project complies with the Spanish law governing assisted reproductive technologies (14/2006).

RESULTS

Phase 1. Analysis of novel morphokinetic parameters

The mean and standard deviation for novel morphodynamical parameters from implanted and non-implanted embryos is shown in Table 1.

Pronuclear migration: Pronuclei from the embryos analyzed travelled distances from 2 to 38 µm. We found non-significant differences between implanted and non-implanted embryos, in terms of distance and speed.

Blastocyst expanded diameter: Blastocysts reached sizes ranging from 114 to 225 µm. Implanted embryos had significantly higher diameters than non-implanted ones. The implantation rate also improved as the ratio BEd/tBEd was higher: 46.2% for ≤1.37, 45.3% for 1.37-1.52, 66.7% for 1.52-1.64 and 70.7% for >1.64.

Inner cell mass area: The ICM assessed ranging from 1 051 to 4 847 μm^2. Non-significant differences were found related to implantation rate. The tendency was the following, embryos with larger ICM areas had better implantation rate. Similar results were found for the ratio ICMa/tICMa: 52.1% for ≤19.07, 61.00% for 19.07-23.87, 63.8% for 23.87-28.90 and 57.4% for >28.90.

Trophectoderm cell cycle length: Trophectoderm cell cycles were shorter than blastomeric cell cycles. Additionally, we found significant differences between implanted and non-implanted embryos.

Phase 2. Development of the predictive model based on ANN

The mean and standard deviation for conventional morphokinetic parameters from implanted and non-implanted embryos is shown in Table 1.

Independent variables capable of discriminating between implanted and non-implanted embryos were: t4, t6, t7, t8, t9, tSC, tM, tSB, tB, tEB, blastocyst expanded diameter and trophectoderm cell cycle length.

After the pre-processing of the dataset, 451 embryos were considered to develop the ANN architecture. The higher predictive power was achieved by ANN3 with an AUC of 0.77 (Figure 2). The results in terms of sensitivity, specificity, accuracy, F-Score and area under the curve for the four models in the testing data set are represented in Table 2.

DISCUSSION

Novel embryo morphodynamical parameters described in this research could play an important role in the implantation potential prediction. Their combination with conventional morphokinetic parameters by using ANNs has resulted in an effective tool to predict the success of an IVF treatment.

Since the introduction of time-lapse systems in IVF laboratories, several algorithms have been developed with morphokinetic parameters to improve embryo evaluation and selection (24,29). The efficacy of six time-lapse imaging embryo selection algorithms to predict implantation (5,25,35,51–53) showed AUCs ranging from 0.543 to 0.629 (54). The insertion of new embryo features and new methodologies of data analysis could improve the predictive power.

The appearance, movement and fading of pronuclei had been previously studied (55–57). Whereas the female pronucleus appears near the second polar body, in the cortex of the oocyte, the male pronucleus can emerge in the center (53.6%), in the cortex (15.2%) or in an intermediate point (31.2%) (55). The central position of PN juxtaposition and the presence of multinucleated blastomeres at 2-cell stage have been associated with the likelihood of live birth when transferring embryos on day 2/3 (57). As a general rule, both pronuclei move together, merge and fade (56). The distance and speed of pronuclei migration before fading were added as input data in our AI model. We did not find an association between implantation rate and multinucleation at 2-cell stage. However, we found the intermediate PN position at juxtaposition was associated with higher clinical pregnancy rate, but the inclusion of this parameter as input variable for ANN did not improve its performance (unpublished data).

According to the ASEBIR criteria and Gardner grading, ICM, blastocyst expansion and trophectoderm are the criteria per excellence to evaluate and select embryos on day 5 of development (Supplemental table 1, Supplemental table 2, Supplemental table 3 and Supplemental table 4). Therefore, we wanted to analyze these parameters in an objective and quantitative way by using measurements of BEd, ICMa and ccTroph

length. Two decades ago, Richter et al. were the first group in demonstrating that embryos with bigger ICM areas had higher implantation rates (58). Although we did not find statistical difference regarding the impact of the ICM size over the implantation potential as independent variable (Table 1), the most predictive ANNs include this parameter (Table 2). The relation between the blastocyst diameter and the clinical outcome was first described through an ocular micrometer in 2008 (59). Although the blastocyst diameter and the ICM dimension had been already assessed with the tools of the Embryo Viewer™ (60), this is the largest retrospective cohort study with time-lapse system including these blastocyst features. In agreement with our results, the transfer of fully expanded blastocysts yielded greater implantation rates in fresh (61,62) and frozen embryo transfers (63). Blastocyst expansion has been also associated with embryo ploidy, as euploid blastocysts usually expand earlier than aneuploid ones (64). To our knowledge, this is the first time that the trophectoderm cell cycle length is measured, although the rapid expansion has been associated with an integrative cellular mitosis in trophectoderm cells (64). To ensure that the ccTroph length was representative of each embryo, we performed the measurement on two different cells for 100 embryos without obtaining significant variations (unpublished data).

The development of AI algorithms has become a common practice in embryological investigations (43). Most of them are focused on image analysis through computer vision. Although, computer vision is a promising tool to use all the data hidden in time-lapse images, it is still improving in the field of human embryology. There is one tool, called STORK, proposed to predict blastocyst quality as an embryologist with high predictive value (AUC=0.98), based on time-lapse images (45). Nevertheless, in their classification, good and bad quality embryos had little difference in the probability to lead a birth, 61.4% and 50.9% respectively. Complete videos of the whole embryo development have also been tested in a software called IVY with high capacity of predicting fetal heart (AUC=0,93) (44). However, the predictive power was calculated using all kind of embryos, even non-viable (7,063 discarded embryos out of 10,683). We are aware that it is an easy population for being classified, also by embryologists. The main goal should be to distinguish among viable embryos with similar appearance, those which have possibility of being transferred.

Currently, there is no doubt that Artificial Intelligence techniques such as ANNs are more powerful than conventional statistical methodologies for data analysis. Among the models of ANN performed in this research, the third one was the most successful. It means that all the characteristics together are more predictive than individually. Additionally, we found that the new parameters analyzed were responsible for the increase in the predictive power for implantation, as the AUC for conventional morphokinetics was 0.64 and 0.77 for their combination with the novel parameters. Also, the accuracy for implantation prediction was higher with new parameters than with conventional ones, 0.75 and 0.71 respectively. Digging deeper into the predictive results, the highest sensitivity was found with those parameters which were significantly different in implanted and non-implanted embryos (Table 2). It means they had higher capacity of discriminating the implanted embryos, but not the non-implanted ones, as the specificity was too low. Thus, the most balanced model was the ANN3, which had the highest specificity and an excellent sensitivity (0.67 and 0.82 respectively).

The predictive value of implantation would be likely higher with the addition of parameters related to the patients. We recognize that the implantation is not only dependent on the embryo quality, the characteristics of the endometrium and the reproductive history also play an important role in the IVF treatments. Regardless of the patient demographics, our further aim is to apply this ANN tool to improve the embryo selection in the laboratory prior to transfer.

We used morphodynamical annotations, which are more consistent, robust and objective than morphological ones (65). However, the inter-observer variability of time-lapse annotations limit the generalizability of our findings and especially with the new described parameters. Additionally, although we used a high-quality TL system supplied with different focal planes, the embryonic three-dimensional morphology made the evaluation of some events difficult, mainly those related to pronuclei. In the near future, these annotations could be performed automatically by using computer vision to reduce the subjectivity. This study is also limited by its retrospective nature, which is necessary before using a new embryo selection model in the IVF laboratory.

CONCLUSION

From our study, we can underline the identification of non-conventional embryo parameters involved in the implantation potential. The use of Artificial Intelligence to analyze big data provided by time-lapse systems, showed that the most predictive model was made up of all the variables described and not only those that were individually discriminatory. The further step will be to compare our model prospectively against standard selection methodologies. We expect that the imminent introduction of new technologies and the resulting use of these morphodynamical parameters may increase the objectivity in embryo evaluation.

ACKNOWLEDGEMENTS

The authors' research is supported by The Ministry of Science, innovation and Universities CDTI (IDI-20191102), Industrial PhD grant (DIN2018-009911) and Agencia Valenciana de Innovació (INNCAD00-18-009) awarded to M.M. and E.P.

We acknowledge the embryologists and technicians of the IVF laboratory from IVI-RMA Global Valencia for their clinical support.

REFERENCES

1. De Geyter C, Calhaz-Jorge C, Kupka MS, Wyns C, Mocanu E, Motrenko T, et al. ART in Europe, 2014: Results generated from European registries by ESHRE. Hum Reprod 2018; 33:1586–601.
2. Edwards RG, Fishel SB, Cohen J, Fehilly CB, Purdy JM, Slater JM, et al. Factors influencing the success of in vitro fertilization for alleviating human infertility. J Vitr Fertil Embryo Transf 1984; 1:3–23.
3. Ferraretti AP, Goossens V, De Mouzon J, Bhattacharya S, Castilla JA, Korsak V, et al. Assisted reproductive technology in Europe, 2008: results generated from European registers by ESHRE. Hum Reprod 2012; 27:2571–84.
4. Zhang JQ, Li XL, Peng Y, Guo X, Heng BC, Tong GQ. Reduction in exposure of human embryos outside the incubator enhances embryo quality and blastulation rate. Reprod Biomed Online 2010; 20:510–5.
5. Cruz M, Garrido N, Herrero J, Pérez-Cano I, Muñoz M, Meseguer M. Timing of

cell division in human cleavage-stage embryos is linked with blastocyst formation and quality. Reprod Biomed Online 2012; 25:371–81.

6. Kirkegaard K, Agerholm IE, Ingerslev HJ. Time-lapse monitoring as a tool for clinical embryo assessment. Hum Reprod 2012; 27:1277–85.

7. Montag M, Liebenthron J, Köster M. Which morphological scoring system is relevant in human embryo development? Placenta 2011; 32:252–6.

8. Aparicio B, Cruz M, Meseguer M. Is morphokinetic analysis the answer? Reprod Biomed Online 2013; 27:654–63.

9. Del Gallego R, Remohí J, Meseguer M, Affiliations A, Valencia IG. Time-Lapse Imaging : The State of the Art . Biol Repod 2019; 101:1146-54

10. Zaninovic N, Irani M, Meseguer M. Assessment of embryo morphology and developmental dynamics by time-lapse microscopy: is there a relation to implantation and ploidy? Fertil Steril 2017; 108:722–9.

11. Wirka KA, Chen AA, Conaghan J, Ivani K. Atypical embryo phenotypes identi fi ed by time-lapse microscopy : high prevalence and association with embryo development. Fertil Steril 2014; 101:1637-1648.e5.

12. Zhan Q, Ye Z, Clarke R, Rosenwaks Z, Zaninovic N. Direct unequal cleavages: Embryo developmental competence, genetic constitution and clinical outcome. PLoS One 2016; 11:1–19.

13. Goodman LR, Goldberg J, Falcone T, Austin C, Desai N. Does the addition of time-lapse morphokinetics in the selection of embryos for transfer improve pregnancy rates? A randomized controlled trial. Fertil Steril 2016; 105:275–85.

14. Desai N, Ploskonka S, Goodman L, Attaran M, Goldberg JM, Austin C, et al. Delayed blastulation, multinucleation, and expansion grade are independently associated with live-birth rates in frozen blastocyst transfer cycles. Fertil Steril 2016; 106:1370–8.

15. Aguilar J, Rubio I, Muñoz E, Pellicer A, Meseguer M. Study of nucleation status in the second cell cycle of human embryo and its impact on implantation rate. Fertil Steril 2016; 106:291–9.

16. Rubio I, Kuhlmann R, Agerholm I, Kirk J, Herrero J. Limited implantation success of direct-cleaved human zygotes : a time-lapse study. Fertil Steril 2012; 98:11–5.

17. Desai N, Ploskonka S, Goodman LR, Austin C, Goldberg J, Falcone T. Analysis of

embryo morphokinetics, multinucleation and cleavage anomalies using continuous time-lapse monitoring in blastocyst transfer cycles. Reprod Biol Endocrinol 2014; 12:54.

18. Ebner T, Höggerl A, Oppelt P, Radler E, Enzelsberger SH, Mayer RB, et al. Time-lapse imaging provides further evidence that planar arrangement of blastomeres is highly abnormal. Arch Gynecol Obstet 2017; 296:1199–205.

19. Azzarello A, Hoest T, Hay-Schmidt A, Mikkelsen AL. Live birth potential of good morphology and vitrified blastocysts presenting abnormal cell divisions. Reprod Biol 2017; 17:144–50.

20. Desch L, Bruno C, Luu M, Barberet J, Choux C, Lamotte M, et al. Embryo multinucleation at the two-cell stage is an independent predictor of intracytoplasmic sperm injection outcomes. Fertil Steril 2017; 107:97-103.e4.

21. Kirkegaard K, Hindkjaer JJ, Grøndahl ML, Kesmodel US, Ingerslev HJ. A randomized clinical trial comparing embryo culture in a conventional incubator with a time-lapse incubator. J Assist Reprod Genet 2012; 29:565–72.

22. Wong CC, Loewke KE, Bossert NL, Behr B, De Jonge CJ, Baer TM, et al. Non-invasive imaging of human embryos before embryonic genome activation predicts development to the blastocyst stage. Nat Biotechnol 2010; 28:1115–21.

23. Conaghan J, Chen AA, Willman SP, Ivani K, Chenette PE, Boostanfar R, et al. Improving embryo selection using a computer-automated time-lapse image analysis test plus day 3 morphology: Results from a prospective multicenter trial. Fertil Steril 2013; 100:412–9.

24. Milewski R, Kuć P, Kuczyńska A, Stankiewicz B, Łukaszuk K, Kuczyński W. A predictive model for blastocyst formation based on morphokinetic parameters in time-lapse monitoring of embryo development. J Assist Reprod Genet 2015; 32:571–9.

25. Chamayou S, Patrizio P, Storaci G, Tomaselli V, Alecci C, Ragolia C, et al. The use of morphokinetic parameters to select all embryos with full capacity to implant. J Assist Reprod Genet 2013; 30:703–10.

26. Milewski R, Czerniecki J, Kuczyńska A, Stankiewicz B, Kuczyński W. Morphokinetic parameters as a source of information concerning embryo developmental and implantation potential. Ginekol Pol 2016; 87:677–84.

27. Motato Y, de los Santos MJ, Escriba MJ, Ruiz BA, Remohí J, Meseguer M. Morphokinetic analysis and embryonic prediction for blastocyst formation through an integrated time-lapse system. Fertil Steril 2016; 105:376–84.
28. Petersen BM, Boel M, Montag M, Gardner DK. Development of a generally applicable morphokinetic algorithm capable of predicting the implantation potential of embryos transferred on Day 3. Hum Reprod 2016; 31:2231–44.
29. Meseguer M, Herrero J, Tejera A, Hilligsøe KM, Ramsing NB, Remoh J. The use of morphokinetics as a predictor of embryo implantation. Hum Reprod 2011; 26:2658–71.
30. Liu Y, Chapple V, Feenan K, Roberts P, Matson P. Time-lapse deselection model for human day 3 in vitro fertilization embryos: The combination of qualitative and quantitative measures of embryo growth. Fertil Steril 2016; 105:656-662.
31. Vermilyea MD, Tan L, Anthony JT, Conaghan J, Ivani K, Gvakharia M, et al. Computer-automated time-lapse analysis results correlate with embryo implantation and clinical pregnancy: A blinded, multi-centre study. Reprod Biomed Online 2014; 29:729–36.
32. Basile N, Vime P, Florensa M, Aparicio Ruiz B, García Velasco JA, Remohí J, et al. The use of morphokinetics as a predictor of implantation: A multicentric study to define and validate an algorithmfor embryo selection. Hum Reprod 2015; 30:276–83.
33. Aparicio-Ruiz B, Romany L, Meseguer M. Selection of preimplantation embryos using time-lapse microscopy in in vitro fertilization: State of the technology and future directions. Birth Defects Res 2018; 110:648–53.
34. Barrie A, Homburg R, McDowell G, Brown J, Kingsland C, Troup S. Preliminary investigation of the prevalence and implantation potential of abnormal embryonic phenotypes assessed using time-lapse imaging. Reprod Biomed Online 2017; 34:455–62.
35. Campbell A, Fishel S, Bowman N, Duffy S, Sedler M, Hickman CFL. Modelling a risk classification of aneuploidy in human embryos using non-invasive morphokinetics. Reprod Biomed Online 2013; 26:477–85.
36. Desai N, Goldberg JM, Austin C, Falcone T. Are cleavage anomalies, multinucleation, or specific cell cycle kinetics observed with time-lapse imaging

predictive of embryo developmental capacity or ploidy? Fertil Steril 2018; 109:665–74.

37. Amir H, Barbash-Hazan S, Kalma Y, Frumkin T, Malcov M, Samara N, et al. Time-lapse imaging reveals delayed development of embryos carrying unbalanced chromosomal translocations. J Assist Reprod Genet 2019; 36:315–24.

38. Del Carmen Nogales M, Bronet F, Basile N, Martínez EM, Liñán A, Rodrigo L, et al. Type of chromosome abnormality affects embryo morphology dynamics. Fertil Steril 2017; 107:229–35.

39. Dyer S, Chambers GM, Mouzon J De, Nygren KG, Mansour R, Ishihara O, et al. International Committee for Monitoring Assisted Reproductive Technologies world report : Assisted Reproductive Technology 2008 , 2009 and 2010. Hum Reprod 2016; 31:1588–609.

40. Simopoulou M, Sfakianoudis K, Maziotis E, Antoniou N, Rapani A, Anifandis G, et al. Are computational applications the “crystal ball” in the IVF laboratory? The evolution from mathematics to artificial intelligence. J Assist Reprod Genet 2018; 35:1545–57.

41. Matusevičius A, Dirvanauskas D, Maskeliūnas R, Raudonis V. Embryo cell detection using regions with convolutional neural networks. CEUR Workshop Proc 2017; 1856:89–93.

42. Milewski Robert, Kuczyńskabc Agnieszka, Stankiewiczb Bożena KW. How much information about embryo implantation potential is included in morphokinetic data? A prediction model based on artificial neural networks and principal component analysis. Adv Med Sci 2017; 62:202–6.

43. Curchoe CL, Bormann CL. Artificial intelligence and machine learning for human reproduction and embryology presented at ASRM and ESHRE 2018. J Assist Reprod Genet 2019; 36:591–600.

44. Tran D, Cooke S, Illingworth PJ, Gardner DK. Deep learning as a predictive tool for fetal heart pregnancy following time-lapse incubation and blastocyst transfer. Hum Reprod 2019; 34:1011–8.

45. Khosravi P, Kazemi E, Zhan Q, Malmsten JE, Toschi M, Zisimopoulos P, et al. Deep learning enables robust assessment and selection of human blastocysts after in vitro fertilization. npj Digit Med 2019; 2:1–9.

46. Cerrillo M, Herrero L, Guillén A, Mayoral M, García-Velasco JA. Impact of Endometrial Preparation Protocols for Frozen Embryo Transfer on Live Birth Rates. Rambam Maimonides Med J 2017; 8.
47. Karsoliya S. Approximating number of hidden layer neurons in multiple hidden layer BPNN architecture. Int J Eng Trends Technol 2012; 3:714–7.
48. Boger Z, Guterman H. Knowledge extraction from artificial neural network models. In 1997 IEEE International Conference on Systems, Man, and Cybernetics. Comput Cybern Simul 1997; 4:3030–5.
49. Panchal G, Ganatra A, Kosta Y., Panchal D. Behaviour analysis of multilayer perceptrons with multiple hidden neurons and hidden layers. Int J Comput Theory Eng 2011; 3:332-7.
50. Kuhn M, Johnson K. Applied predictive modeling. New York Springer 2013.
51. Azzarello A, Hoest T, Mikkelsen AL. The impact of pronuclei morphology and dynamicity on live birth outcome after time-lapse culture. Hum Reprod 2012;27:2649–57.
52. Basile N, Vime P, Florensa M, Aparicio Ruiz B, García Velasco JA, Remohí J, et al. The use of morphokinetics as a predictor of implantation: A multicentric study to define and validate an algorithmfor embryo selection. Hum Reprod 2015; 30:276-83
53. Dal Canto M, Coticchio G, Mignini Renzini M, De Ponti E, Novara PV, Brambillasca F, et al. Cleavage kinetics analysis of human embryos predicts development to blastocyst and implantation. Reprod Biomed Online 2012; 25:474–80.
54. Barrie A, Homburg R, McDowell G, Brown J, Kingsland C, Troup S. Examining the efficacy of six published time-lapse imaging embryo selection algorithms to predict implantation to demonstrate the need for the development of specific, in-house morphokinetic selection algorithms. Fertil Steril 2017; 107:613–21.
55. Coticchio G, Renzini MM, Novara P V., Lain M, Ponti E De, Turchi D, et al. Focused time-lapse analysis reveals novel aspects of human fertilization and suggests new parameters of embryo viability. Hum Reprod 2018; 33:23–31.
56. Aguilar J, Motato Y, Escribá MJ, Ojeda M, Muñoz E, Meseguer M. The human first cell cycle: Impact on implantation. Reprod Biomed Online 2014; 28:475–84.

57. Barberet J, Bruno C, Valot E, Jonval L, Chammas J, Choux C, et al. Can novel early non-invasive biomarkers of embryo quality be identified with time-lapse imaging to predict live birth ? Hum Reprod Update 2019; 34:1439–49.
58. Richter KS, Harris DC, Daneshmand ST, Shapiro BS. Quantitative grading of a human blastocyst: Optimal inner cell mass size and shape. Fertil Steril 2001; 76:1157–67.
59. Shapiro BS, Daneshmand ST, Garner FC, Sc M. Large blastocyst diameter , early blastulation , and low preovulatory serum progesterone are dominant predictors of clinical pregnancy in fresh autologous cycles. Fertil Steril 2008; 90:302-9.
60. Almagor M, Harir Y, Fieldust S, Or Y, Shoham Z. Ratio between inner cell mass diameter and blastocyst diameter is correlated with successful pregnancy outcomes of single blastocyst transfers. Fertil Steril 2016; 106:1386–91.
61. della Ragione T, Verheyen G, Papanikolaou EG, Landuyt L Van, Devroey P, Steirteghem A Van. Developmental stage on day-5 and fragmentation rate on day-3 can influence the implantation potential of top-quality blastocysts in IVF cycles with single embryo transfer. Reprod Biol Endocrinol 2007; 8:1–8.
62. Shapiro BS, Harris DC, Richter KS, Ph D. Predictive value of 72-hour blastomere cell number on blastocyst development and success of subsequent transfer based on the degree of blastocyst development. Fertil Steril 2000; 73:10–3.
63. Coello A, Meseguer M, Galán A, Alegre L, Remohí J, Cobo A. Analysis of the morphological dynamics of blastocysts after vitrification/warming: defining new predictive variables of implantation. Fertil Steril 2017; 108:659-666.e4.
64. Huang TT, Huang DH, Ahn HJ, Arnett C, Huang CT. Early blastocyst expansion in euploid and aneuploid human embryos: evidence for a non-invasive and quantitative marker for embryo selection. Reprod Biomed Online 2019; 39:27–39.
65. Sundvall L, Ingerslev HJ, Breth Knudsen U, Kirkegaard K. Inter- and intra-observer variability of time-lapse annotations. Hum Reprod 2013; 28:3215–21.

FIGURE LEGENDS

Figure 1. Measurement methodology carried out with the drawing tools provided by the EmbryoViewer™ (Vitrolife, Denmark). A) Measurement of pronuclear (PN) migration; the image on the right represents the initial migration point and the image on the left represents the distance travelled by pronuclei at the end migration point. B) Measurement of blastocyst expanded diameter. C) Measurement of Inner Cell Mass Area. D) Measurement of trophectoderm cell cycle length; the image on the right represents the selected trophectoderm cell, the next image represents the two daughter cells from the selected cell, and the image on the left represents the four daughter cells from the two cells of the previous image.

Figure 2. ROC curve for prediction of implantation on the testing dataset by ANN3 (conventional morphokinetic and novel parameters as input data). ROC, Receiver operating characteristic. AUC, area under the curve.

TABLES

Table 1. Mean and standard deviation for each embryo parameter analyzed. The p value shows the statistical differences between implanted and non-implanted embryos. PNm, pronuclear migration; BEd, blastocyst expanded diameter; ICMa, inner cell mass area; ccTroph, trophectoderm cell cycle; tBEd, the time from ICSI to BEd measurement; tICMa, the time from ICSI to ICMa measurement.

Table 2. Results obtained in terms of sensitivity, specificity, accuracy, F-Score and AUC for each ANN model on testing data set. ANN, artificial neural network; AUC, area under the curve; tpb2, the time of the second polar body emission; tPNa the time of appearance of the two pronuclei; tPNf, the time of their fade out; t2, the division time to two cells; t3, the division time to three cells; t4, the division time to four cells; t5, the division time to five cells; t6, the division time to six cells; t7, the division time to seven cells; t8, the division time to eight cells; tSC, the time from ICSI to early compaction; tM, the time from ICSI to morula formation; tSB, the time from ICSI to early blastulatio; tB, the time from ICSI to full blastocyst; tEB, the time from ICSI to expanded blastocyst; and tHiB, the time from ICSI to to early hatching blastocyst; PNm, pronuclear migration, BEd, blastocyst expanded diameter; ICMa, inner cell mass area; ccTroph, trophectoderm cell cycle.

OTHER LEGENDS

Supplemental table 1. Categories and characteristics of embryonic inner cell mass according to the ASEBIR criteria 2015.

Supplemental table 2. Categories and characteristics of trophectoderm according to the ASEBIR criteria 2015.

Supplemental table 3. Embryo classification on day 5 of development, according to the ASEBIR criteria 2015, based on expansion grade, inner cell mass (ICM) and trophectoderm quality.

Supplemental table 4. Gardner's system for grading human blastocysts on day 5 of development.

Supplemental figure 1. Scheme of the designed architecture of Artificial Neural Network, where m is the number of input variables and h is the number of neurons in the hidden layers.

FIGURES AND TABLES

Figure 1.

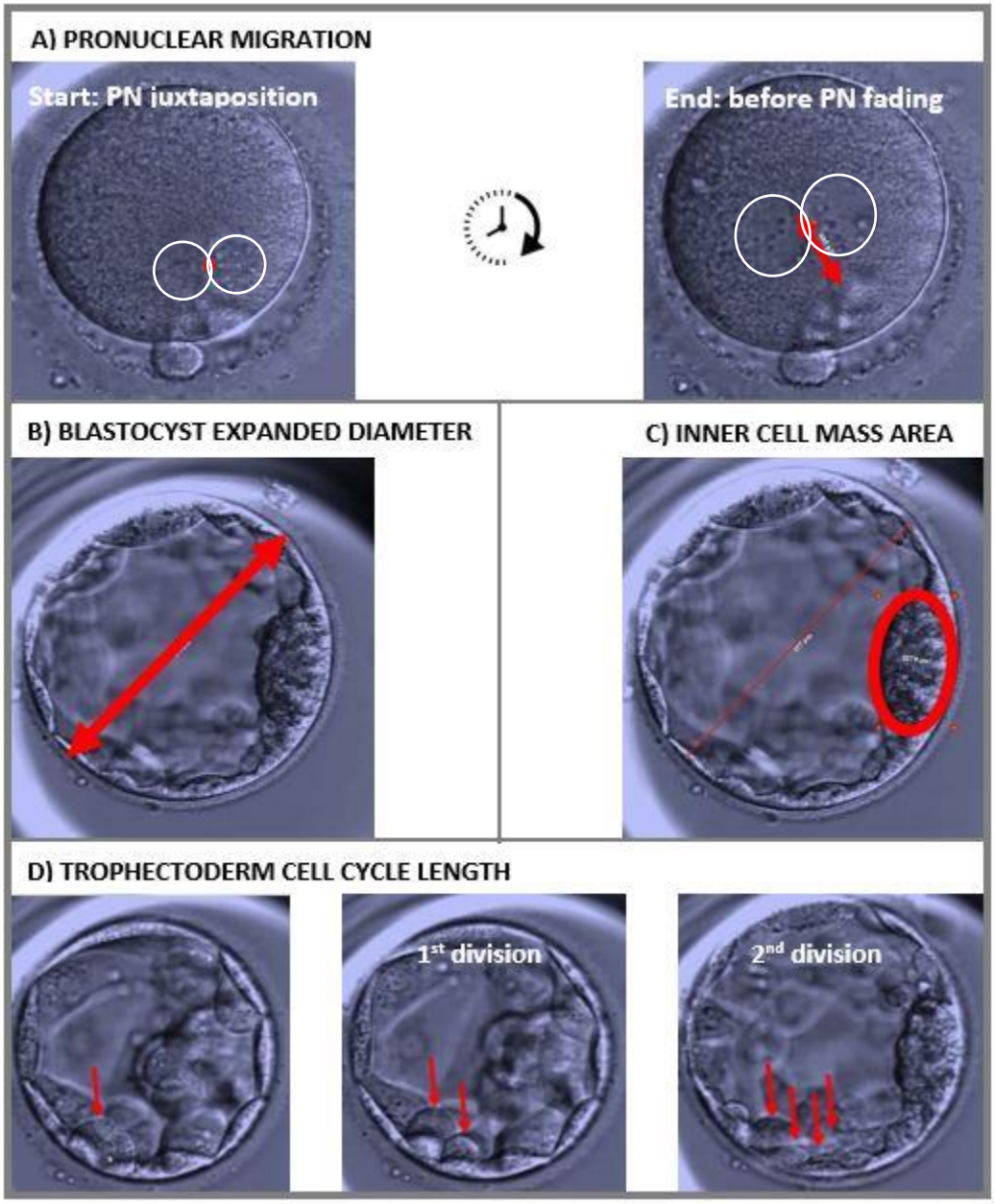

Figure 2.

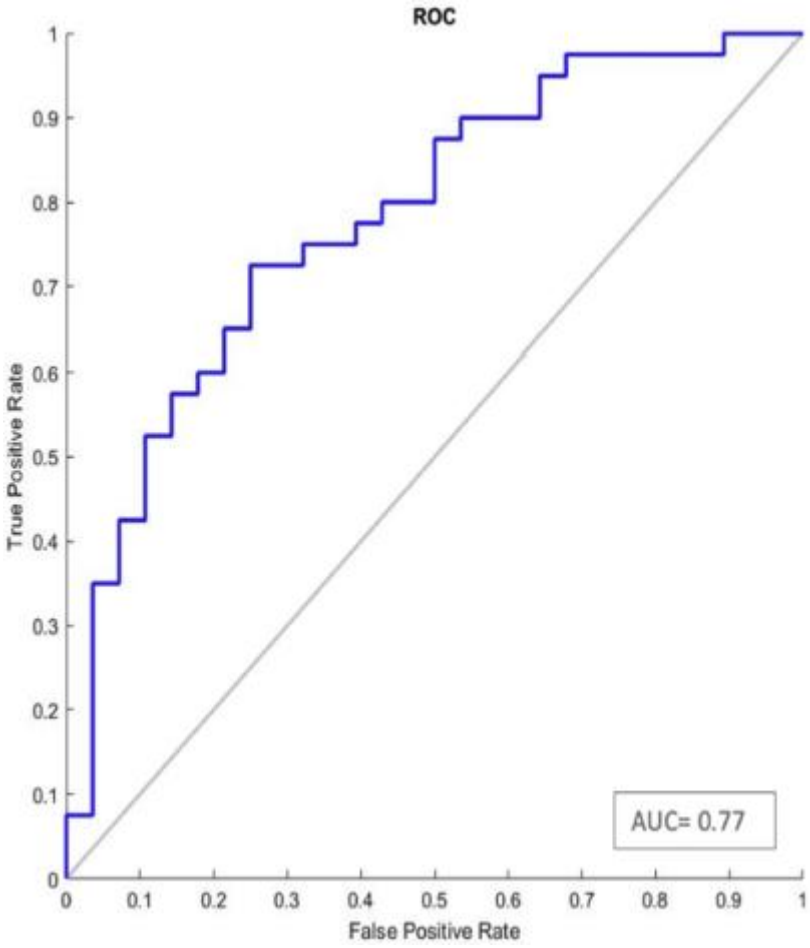
ROC
True Positive Rate
False Positive Rate
AUC= 0.77
0
0.1
0.2
0.3
0.4
0.5
0.6
0.7
0.8
0.9
1

Table 1.

Variable	Unit (SI)	Implanted embryos		Non-implanted embryos		P value
		Mean	Standard deviation	Mean	Standard deviation	
tPB2	h	3.763	1.425	3.858	1.585	0.907
tPNa	h	8.559	2.187	8.735	2.283	0.926
tPNf	h	23.192	2.559	23.508	2.745	0.194
t2	h	25.654	2.956	25.951	2.973	0.383
t3	h	36.219	3.361	36.500	3.817	0.356
t4	h	37.403	3.663	38.154	3.975	0.031*
t5	h	48.801	5.109	49.104	5.812	0.526
t6	h	50.386	5.006	51.519	5.779	0.023*
t7	h	52.777	5.464	54.468	7.031	0.009*
t8	h	56.607	7.817	59.840	10.137	0.003*
t9	h	69.889	8.209	72.800	8.635	<0.001*
tSC	h	80.891	8.757	83.139	9.163	0.012*
tM	h	86.925	8.265	88.689	8.591	0.017*
tSB	h	96.843	6.712	98.978	6.979	0.001*
tB	h	102.436	6.740	104.326	7.216	0.005*
tEB	h	107.940	6.452	110.274	6.592	0.001*
tHiB	h	110.638	7.694	114.796	9.790	0.418
Distance PNm	µm	13.649	7.234	13.648	6.898	0.936
Speed PNm	µm/h	1.377	1.989	1.174	0.995	0.079
BEd	µm	177.090	21.374	170.830	18.575	<0.001*
ICMa	μm^2	2763.036	707.134	2716.188	830.591	0.069
ccTroph	h	9.945	2.706	9.758	2.702	<0.001*
tICMa	h	113.369	5.419	114.252	9.046	0.184
tBEd	h	113.527	3.787	113.637	2.915	0.461

*p<0.05; statistically significant differences for the mean value between implanted and non-implanted embryos.

1 Table 2.

2

Artificial Neural Network	Input Data	Sensitivity	Specificity	Accuracy	F-Score	AUC
ANN1	tpb2, tPNa, tPNf, t2, t3, t4, t5, t6, t7, t8, tSC, tM, tSB, tB, tEB, tHiB	0.88	0.46	0.71	0.78	0.64
ANN2	Distance of PNm, speed of PNm, BEd, ICMa, ccTroph	0.86	0.58	0.75	0.80	0.73
ANN3	tpb2, tPNa, tPNf, t2, t3, t4, t5, t6, t7, t8, tSC, tM, tSB, tB, tEB, tHiB, distance of PNm, speed of PNm, BEd, ICMa, ccTroph length	0.82	0.67	0.76	0.80	0.77
ANN4	t4, t6, t7, t8, t9, tSC, tM, tSB, tB, tEB, Bed, ccTroph length	0.85	0.57	0.74	0.79	0.68